Chapter 4

Experimental test preparation, performance and data processing

4.1 Introduction

This chapter is dedicated to the experimental test preparation, performance, and data processing and analysis. Firstly, a review of the basic concepts and terminology related to experimentation, errors, and uncertainty analysis is presented. Because of the diverse nomenclature and terminology used in different literature sources, an attempt is made to review and systemize definitions of errors and uncertainties in experimental measurements. A definition of the terminology and nomenclature adopted in this work is given. The preparation of the experimental tests is described from the point of view of the instruments calibration and the determining of the systematic uncertainties of the individual measuring instruments. The systematic uncertainties of the factory calibrated instruments are described. The specific process of calibration of the temperature sensors is explained. A procedure for the experimental evaluation of the remaining systematic uncertainties of the temperature sensors (RTDs, TCs) is developed and exposed in detail.
A section is dedicated to the experimental results obtained from the measured variables. The evaluation of the cooling capacity of the tested fin-and-tube heat exchangers, independently from the air- and refrigerant-side, is presented. The methods for obtaining the cooling capacity refrigerant-side are explained for the cases when liquid and phase-changing refrigerant is used. Two different modes of testing of liquid overfeed evaporators are regarded. The evaluation of the condenser capacity and the compressor work in the liquid overfeed refrigeration system is also presented. The way of verifying the experimental results through energy balance checks is also described.

The formulation and the methodology adopted for the uncertainty analysis of the experimental results is exposed in detail. Starting from the data reduction equation, the uncertainty propagation equation is obtained. Following a numerical procedure, the partial derivatives (sensitivity coefficients) of the results with respect to each variable are determined. The systematic and the random uncertainties are treated separately and, finally, the overall uncertainty of the result is obtained. Considerations about correlation of systematic uncertainties have been made, based on observations of the behaviour of the sensors through measurements in controlled ambient.
Finally, the experimental processing and analysis is exposed. It has been performed automatically with a specially developed for this purpose computer program. Starting from the pre-processed experimental data for each test point, the program calculates the experimental results, performs the detailed uncertainty analysis, and verifies the experimental results through balance checks, following the previously exposed formulation and methodology. The program is also encharged with the experimental to numerical comparisons, with the objective of experimental validation of the numerical models. It generates an extensive output in tabular and graphical form. The output is presented also in terms of standard deviations of the differences between the numerical and experimental results, as a whole, and for groups divided according to established criteria, permitting quantitative evaluation of the results.

4.2 Concepts and terminology

When experimentation is used to find a solution to a problem, there always exists the need to know how accurate the obtained result is. The word accuracy is generally used to indicate the closeness between the experimentally determined value of a quantity and its true value. Error is defined as the difference between the experimentally determined value of and its true value. As the error decreases, accuracy is said to increase.
Total error (δ) can be considered to be composed of two components: a random (precision or repeatability) component (ϵ) and a systematic (bias or fixed) component (β). An error is classified to be random if it contributes to a scatter of the data; otherwise, it is systematic error. It is assumed that corrections have been made for all systematic errors whose values are known. The remaining random errors are thus equally likely to be positive or negative.
As the true value of a measured quantity is never known, we are forced to estimate the error of the measurement and this estimate is called an uncertainty (U). Uncertainty estimates are made at some confidence level. Usually a 95% confidence estimate is adopted, what means that the true value of the quantity is expected to be within the $\pm U$ interval about the experimentally determined value 95 times out of 100.
The nomenclature and the terminology used in literature concerning experimental

measurement uncertainty analysis unfortunately has not been consistent. Terms as bias, precision, bias limit, precision index are used in some works, while systematic and random uncertainy are used in others. This may give place to an ambiguity and confusion, and an intent to avoid this is made with the following overview of definitions and comments.

As defined by Coleman et al.[1] the bias error (β) is "the fixed, systematic, or constant component of the total error and is sometimes referred to simply as bias". The precision error (ϵ) "is the random component of the total error and is sometimes called the repeatability or repeatability error".

Moffat [2], in agreement with [1], defines the bias limit of a measurement as an estimate of the maximum probable value of the fixed error, usually estimated at 95% confidence. The precision index of a measurement is defined as a measure of its random error. The precision index of a data set is equal to its standard deviation s_{Xi}, and can be estimated from the test data alone without an external reference. If a value is determined as a mean from a data set of N readings, the standard deviation of the mean is used $S_{\bar{X}i}$=$s_{Xi}/\sqrt{N}$. To be useful in estimating uncertainty, an appropriate value of the Student's t multiplier can be used to describe 95% confidence interval for the measured value.

In 1993 the ISO Guide [3] was published in the name of seven international organizations, establishing general rules for evaluating and expressing uncertainty in measurements. The ISO Guide accepts the use of the terms systematic and random error, denominating thus respectively the bias and the precision errors, but adopts classification of the uncertainties by the source of information about them. The uncertainties are divided into type A and type B uncertainties instead of systematic and random. Type A uncertainties are those evaluated "by the statistical analysis of series of observations" whereas type B uncertainties are those evaluated "by means other than the statistical analysis of series of observation". Types A and B unambiguously define how an uncertainty estimate was made. This classification is to indicate the two different ways of evaluating uncertainty components and is not meant to indicate that there is any difference in the nature of the components resulting from the two types of evaluation. Both types of evaluation are based on probability distributions, and the uncertainty components resulting from either type are quantified by variances or standard deviations.

The Test Uncertainty Supplement of the ASME Standard PTC19.1-1998 [4] published in december 1998 adopts classification of the uncertainties considering their effect on the measured result, in difference with the ISO Guide. That is, if an uncertainty source causes scatter in test result, it is a random uncertainty source and has been caused by random errors. If not, it is a systematic uncertainty and has been caused by systematic errors. The use of terms as bias limit and precision index is eliminated. These recognizable terms are treated as follows. The term bias limit, meaning the

estimated limits of the error caused by bias error sources, is described by the term systematic uncertainty. The term precision, meaning the estimate of the magnitude of error caused by precision error sources, is described by the term random uncertainty. The term precision index has been changed to the standard deviation of the mean. The harmonization of PTC19.1-1998 [4] with the ISO Guide [3] is achieved by recommending a simplified root-sum-square (RSS) uncertainty model. Several simplifying assumptions have been made. All systematic uncertainty sources are assumed normally distributed and are estimated as 2σ for 95% coverage. All random uncertainty sources are estimated as $2S_{\bar{X}}$, which is a 95% confidence estimate of the effect on the average of a particular random uncertainty source. These uncertainty estimates are grouped as systematic or random and root-sum-squared to obtain the systematic and random uncertainties of a measurement, B and $2S_{\bar{X}}$ for large samples ($N > 30$). These are then root-sum-squared to obtain a 95% confidence uncertainties: $U = [B^2 + (2S_{\bar{X}})^2]^{1/2}$.
The previous overview manifests that although adopting similar mathematical procedures the actual uncertainty analysis uses two different classifications for the uncertainties: by the source of information about them and by their effect on the measured result. In this thesis the most commonly used classification for uncertainties by their effect as systematic/random is adopted, considering its tradition in engineering and its usefulness in the estimation of the expected dispersion of the results for a particular experiment. Hereafter the term random uncertainty will be used for the estimated limits of errors produced by random error sources and the term systematic ucertainty will be used for the estimated limits of the error caused by systematic error sources. The term accuracy of a measuring instrument (usually provided by the manufacturer) is interpreted and used as a systematic uncertainty in the measurement of that instrument for the purpose of the uncertainty analysis.

4.3 Calibration and test procedures

The calibration is the act of checking or adjusting the accuracy of a measuring instrument by comparison with a standard. Most of the instruments used in the experiment, as flow-meters and pressure transducers are factory calibrated to the range of the measured variables with accuracies stated by the manufacturer in the corresponding calibration certificate. The manufacturer's specifications have been interpreted and converted into an estimate of the equivalent standard deviation (σ) that also describes the data. All the systematic uncertainties obtained from manufacturer's specifications have been converted in 95% confidence estimates in the form $B_{cal} = 2\sigma$. The output signals of the instruments (usually current 4-20 mA or voltage 0-10V) are converted, acquired, conditioned and stored by the data acquisition system. The uncertainties from conversion, data acquisition, and computational resolution have been added to

the manufacturer's calibration uncertainties using the root-sum-square to obtain the systematic uncertainty for each measured variable as given:

$$B_i = \left[(B_{cal})^2 + (B_{acq})^2\right]^{1/2} \tag{4.1}$$

The temperature sensors: resistance thermal devices (RTD, Pt100) and thermocouples (TC) are calibrated in the CTTC following specially developed procedure, using as a reference a platinum resistance precision thermometer having separate acquisition system, with overall accuracy $\pm 0.03^o$C.
The temperature sensors are calibrated individually or in groups, collocating them in an isothermal bath close to the precision thermometer. Only sensors of the same type (RTD or TC) are calibrated simultaneously. The procedure is the following: The temperature sensors are submerged in the isothermal bath together with the precision thermometer close to each other and 30 minute records of their readings are taken in steps of 5^oC from the low to the high calibration range limits.
Calibration curve referencing the reading of each sensor with the reading of the precision thermometer is generated, using the average values of the records for each calibration point, and incorporated in the data acquisition program. Through it the readings of the instruments are corrected to that of the precision thermometer.
The systematic uncertainty after the calibration of the temperature sensors has been determined experimentally. Calibration check is performed after the calibration corrections have been introduced in the data acquisition program, before and after the tests, and this data is used to estimate the remaining systematic uncertainty of the sensors. The readings of the sensors are compared against the readings of the precision thermometer in the isothermal bath. Thirty minute tests are done in points between the calibration points. The mean values of the readings of the precision thermometer and each (i-th) sensor, for each calibration check point are calculated, together with their standard deviations:

$$\bar{T}_i = \frac{1}{N}\sum_{k=1}^{N}(T_i)_k \tag{4.2}$$

$$s_{Ti} = \left[\frac{1}{N-1}\sum_{k=1}^{N}\left[(T_i)_k - \bar{T}_i\right]^2\right]^{\frac{1}{2}} \tag{4.3}$$

$$\bar{T}_{pr} = \frac{1}{N}\sum_{k=1}^{N}(T_{pr})_k \tag{4.4}$$

$$s_{Tpr} = \left[\frac{1}{N-1}\sum_{k=1}^{N}\left[(T_{pr})_k - \bar{T}_{pr}\right]^2\right]^{\frac{1}{2}} \tag{4.5}$$

The standard deviations of the mean are:

$$S_{\bar{T}i} = \frac{s_{Ti}}{\sqrt{N}} \tag{4.6}$$

$$S_{\bar{T}pr} = \frac{s_{Tpr}}{\sqrt{N}} \tag{4.7}$$

where N is the number of measurements in the sample.
Normal distribution of the sample mean values is assumed. The standard deviation of the temperature difference between the mean values measured by the precision thermometer and each sensor can be calculated as:

$$S_i^{diff} = (S_{\bar{T}pr}^2 + S_{\bar{T}i}^2)^{1/2} \tag{4.8}$$

The 95% systematic uncertainty for all temperature sensors of the same type (RTD or TC) is estimated in a conservative manner, using the maximum temperature difference with the precision thermometer found among all the sensors of the same type, and for all check points, and is expressed as:

$$B_i = \left[\left[|\bar{T}_{pr} - \bar{T}_i|_{max} + 2S_i^{diff} \right]^2 + B_{pr}^2 \right]^{1/2} \tag{4.9}$$

where B_i represents the overall systematic uncertainty after calibration, taking account intrinsically for acquisition and calibration curve approximation errors. The first term on the right in (4.9) is composed of the maximum error (not corrected difference with the precision thermometer), found among all the sensors of the same type, augmented with $2S_i^{diff}$, which represents the 95% confidence interval for that error. The second term B_{pr} is the accuracy of the precision thermometer. The continuous comparisons and checks have shown that the overall systematic uncertainty of the K-type thermo-couples after calibration is less than $\pm 0.3^oC$. The systematic uncertainty in the calibrated RTD has proven to be less than $\pm 0.08^oC$.
The stated uncertainties for the RTDs and the TCs are obtained from combining systematic and random uncertainties due to the variation of the temperature in the isothermal bath during the calibration (see eq.(4.9)), but they are "fossilized" into a systematic uncertainty that cannot cause scatter on repeated readings, having obtained them during the calibration, previously to the experiment itself, [2].
Once the calibration of the measuring instruments is concluded and calibration corrections are introduced in the data acquisition program, the experimental tests are performed. The tests are run at stable conditions, normally within time intervals of 30 to 60 minutes, with time-step of data recording approximately 5 seconds. The experimental test record contains more than 300 entries for the variables of interest and could be considered as a large sample for the purpose of the uncertainty analysis.

4.4 Obtaining of the experimental results

The result aimed with the experimentation is mainly the experimental determining of the heat transfer in the tested heat exchanger prototypes, and the components of the liquid overfeed refrigeration system. These magnitudes are obtained from the averaged values of the variables measured during the test in steady state conditions. The usual test duration is between 30 and 60 minutes. The used instrumentation permits the determining of the cooling capacity independently both on the air- and refrigerant-side, using energy balances over the air and the refrigerant. The same is done for the liquid cooled condenser. The refrigerant-side cooling capacity is determined in different ways when liquid and phase-changing refrigerant is used. The formulation used for each case is described subsequently.

4.4.1 Cooling capacity of the air-cooler: air-side

The cooing capacity air-side has been determined from the averaged values of the variables measured during the experimental test. The measured variables and the calculated from them variables, necessary for the calculation of the cooling capacity, are presented as follows:

Measured variables air-side:

T_{ai}	air inlet mean temperature [^{o}C]
T_{ao}	air outlet mean temperature [^{o}C]
ϕ_i	air inlet relative humidity [%]
$\dot{m}_{ao}$	air outlet mass flow-rate [kg/s]
$\dot{m}_w$	condensed water mass flow-rate [kg/s]
p_{abs}	air pressure [Pa]

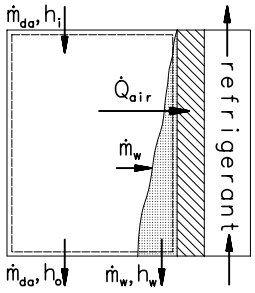

Figure 4.1: Air energy balance terms

Calculated variables air-side:

$W_i = f(T_{ai}, \phi_i, p_{abs})$	air inlet humidity ratio [$kg_w/kg_{d.air}$], [5]
$\dot{m}_{da} = (\dot{m}_{ao} + \dot{m}_w)/(1 + W_i)$	dry air mass flow-rate [kg/s]
$W_o = W_i - (\dot{m}_w)/(\dot{m}_{da})$	air outlet humidity ratio [$kg_w/kg_{d.air}$]
$h_i = f(T_{ai}, W_i)$	air inlet mean specific enthalpy [J/kg], [5]
$h_o = f(T_{ao}, W_o)$	air outlet mean specific enthalpy [J/kg], [5]
$h_w = f(T_w)$	specific enthalpy of liquid water [J/kg], [6]

From energy balance over the air the cooling capacity air-side is obtained:

$$\dot{Q}_{air} = \dot{m}_{da}(h_i - h_o) - \dot{m}_w h_w \tag{4.10}$$

4.4.2 Cooling capacity of the air-cooler: liquid refrigerant-side

The cooing capacity refrigerant-side when using liquid refrigerant is calculated from the averaged values of the variables during the steady state test.

Measured variables liquid-side:

T_{li}	liquid inlet temperature [^{o}C]
T_{lo}	liquid outlet temperature [^{o}C]
$\dot{m}_{liq}$	liquid mass flow-rate [kg/h]
p_{liq}	liquid pressure [Pa]

Calculated variables liquid-side:

$\bar{c}_p \approx f(0.5(T_{li} + T_{lo}))$ liquid average heat capacity [J/kg.K], [6]

From an energy balance over the liquid refrigerant the cooling capacity refrigerant-side when using liquid refrigerant is obtained:

$$\dot{Q}_{liq} = \dot{m}_{liq}\bar{c}_p(T_{lo} - T_{li}) \tag{4.11}$$

4.4.3 Cooling capacity of the evaporator: refrigerant-side

The phase-changing refrigerant circuit presented in section 3.4 permits two different modes of testing liquid overfeed evaporators. In the first mode evaporators are tested as part of the vapour-compression refrigeration system. In the second mode, direct connection between the evaporator and the condenser is used, achieving the adjustment of the evaporating temperature with the secondary fluid in the condenser, without using the compressor. In Figure 4.2 is presented a scheme of the experimental circuit. The vapour-compression refrigeration system with liquid overfeed of the evaporator is represented with continuous line. In this mode the cooling capacity of the evaporator is determined from energy balances over the low-pressure receiver and the evaporator, using the average values of the measured variables during the test in steady state conditions (stable temperatures, pressures, fluxes and refrigerant levels in both receivers, oil recovery closed ($\dot{m}_3 = 0$)). The different points of the system, where variables are measured or calculated in order to make energy balances, are indicated with numbers on the scheme.
The circuit for testing the evaporator without compressor is represented with dashed line in Figure 4.2. In this mode, a direct connection between the evaporator and the condenser is made. The set-up is arranged in a manner that heat to the system is transferred only in the evaporator and the condenser. A liquid refrigerant from

the receiver is provided to the evaporator by means of the pump. The liquid-vapour refrigerant mixture leaving the evaporator is send to the condenser, where the vapour fraction is condensed versus the secondary fluid, and the refrigerant is drained in the receiver. The cooling capacity of the evaporator in this mode is obtained from an energy balance over the secondary fluid in the condenser, taking into account the estimated heat transmitted through the insulated lines connecting the evaporator and the condenser.

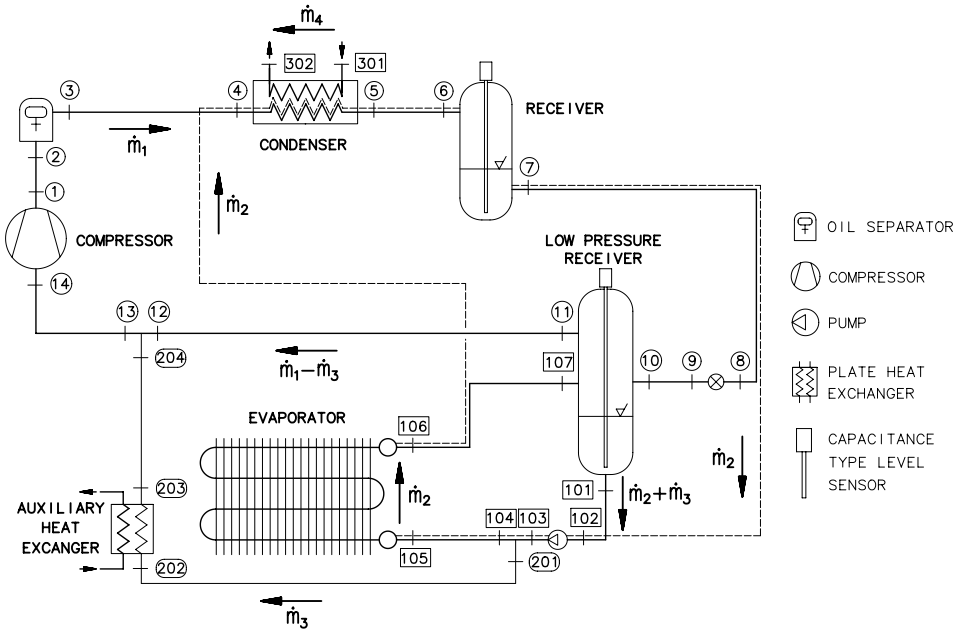

Figure 4.2: Liquid Overfeed Refrigeration Test Facility

The formulation for determining the cooling capacity of the liquid overfeed evaporator in the two modes of testing (with the vapour-compression cycle and without compressor) is herewith presented.

Testing of the evaporator as a part of the refrigeration cycle

Measured variables:

$\dot{m}_2$	refrigerant flow through evaporator [kg/s]
$\dot{m}_1$	refrigerant flow through compressor [kg/s]
T_{105}	refrigerant inlet temperature [^{o}C]
p_{105}	refrigerant inlet pressure [Pa]
T_{106}	refrigerant outlet temperature [^{o}C]
Δp_e	refrigerant pressure drop through evaporator [Pa]
T_8	liquid refrigerant temperature [^{o}C]
p_8	system's high absolute pressure [Pa]
T_{11}	refrigerant vapour to compressor temperature [^{o}C]
p_{11}	system's low absolute pressure [Pa]
T_{102}	liquid refrigerant temperature [^{o}C]
T_1	compressor discharge temperature [^{o}C]
T_4	condenser inlet temperature [^{o}C]
T_5	condenser outlet temperature [^{o}C]
T_{202}	refrigerant temperature [^{o}C]
T_{203}	refrigerant temperature [^{o}C]
H_{lpr}	liquid level low-pressure receiver [mm]
H_{hpr}	liquid level high-pressure receiver [mm]
T_{amb}	ambient temperature [^{o}C]
T_{clim}	climatic chamber temperature [^{o}C]

Estimated variables:

$\dot{Q}_9$	heat gains through tubes between points 8 and 10, [W]
$\dot{Q}_{106}$	heat gains through tubes between points 106 and 107, [W]
$\dot{Q}_{lpr}$	heat gains in the low-pressure receiver, [W]

Calculated variables:

$p_{106} = p_{105} - \Delta p_e$	refrigerant outlet pressure [Pa]
$h_{101} = f(T_{11}, p_{11} + \rho g H_{lpr})$	liquid refrigerant enthalpy [J/kg], REFPROP, [7]
$h_{105} = f(T_{105}, p_{105})$	liquid refrigerant enthalpy [J/kg], REFPROP
$h_8 = f(T_8, p_8)$	liquid refrigerant enthalpy [J/kg], REFPROP
$h_{11} = f(T_{11}, p_{11})$	vapour refrigerant enthalpy [J/kg], REFPROP
$h_{10} = h_8 + \dot{Q}_9/\dot{m}_1$	enthalpy [J/kg], from energy balance
$h_{107} = h_{106} + \dot{Q}_{106}/\dot{m}_2$	enthalpy [J/kg], from energy balance

From energy balance over the low-pressure receiver and substituting h_{107} and h_{10} with their corresponding expressions cited above, the enthalpy at the outlet of the evaporator is obtained:

$$h_{106} = \frac{\dot{m}_1}{\dot{m}_2}(h_{11} - h_{10}) + h_{101} - \frac{1}{\dot{m}_2}(\dot{Q}_{106} + \dot{Q}_{lpr}) \tag{4.12}$$

The cooling capacity of the evaporator is then calculated:

$$\dot{Q}_e = \dot{m}_2(h_{106} - h_{105}) \tag{4.13}$$

The vapour quality at the outlet of the evaporator is calculated from the pressure and the enthalpy using REFPROP program, [7]:

$$x_{g106} = f(p_{106}, h_{106}) \tag{4.14}$$

Testing of the evaporator without compressor

Measured variables:

$\dot{m}_4$	secondary fluid flow in the condenser [kg/s]
T_{301}	inlet temperature of the secondary fluid in the condenser [^{o}C]
T_{302}	outlet temperature of the secondary fluid in the condenser [^{o}C]
$\dot{m}_2$	refrigerant flux through evaporator [kg/s]
T_{105}	refrigerant inlet temperature [^{o}C]
p_{105}	refrigerant inlet pressure [Pa]
T_{106}	refrigerant outlet temperature [^{o}C]
Δp_e	refrigerant pressure drop through evaporator [Pa]
T_{102}	liquid refrigerant temperature [^{o}C]
T_4	condenser inlet temperature [^{o}C]
T_5	condenser outlet temperature [^{o}C]
T_{amb}	ambient temperature [^{o}C]
T_{clim}	climatic chamber temperature [^{o}C]

Estimated variables:

$\dot{Q}_{ev/cd}$	heat gains in refrigerant lines between evaporator and condenser, [W]

Calculated variables:

$p_{106} = p_{105} - \Delta p_e$	refrigerant outlet pressure [Pa]
$\bar{c}_p \approx f(0.5(T_{301} + T_{302}))$	secondary fluid average heat capacity [J/kg.K], [6]

The cooling capacity of the evaporator is determined from an energy balance over the secondary fluid in the condenser, considering the estimated heat gains in the refrigerant lines connecting the evaporator and the condenser:

$$\dot{Q}_e = \dot{m}_4 \bar{c}_p (T_{302} - T_{301}) - \dot{Q}_{ev/cd} \tag{4.15}$$

The enthalpy at the outlet of the evaporator is determiner from:

$$h_{106} = h_{105} + \frac{\dot{Q}_e}{\dot{m}_2} \tag{4.16}$$

The vapour quality at the outlet of the evaporator is calculated from the pressure and the enthalpy using REFPROP program, [7]:

$$x_{g106} = f(p_{106}, h_{106}) \tag{4.17}$$

4.4.4 Condenser capacity: refrigerant-side

The condenser capacity is determined from the measured variables in the R134a refrigerant circuit, Figure 4.2.

Measured variables:

T_4	condenser inlet temperature [^{o}C]
T_5	condenser outlet temperature [^{o}C]
$\dot{m}_1$	refrigerant flow through condenser [kg/s]
p_8	system's high absolute pressure [Pa]

Estimated variables: Pressure losses in condenser and tubes

Calculated variables:

$h_4 = f(T_4, p_4)$	vapour refrigerant enthalpy [J/kg], REFPROP, [7]
$h_5 = f(T_5, p_5)$	liquid refrigerant enthalpy [J/kg], REFPROP

The condenser capacity is determined from:

$$\dot{Q}_{cd} = \dot{m}_1 (h_4 - h_5) \tag{4.18}$$

4.4.5 Condenser capacity: secondary fluid-side

The condenser capacity on the secondary fluid-side is determined from the measured variables (see Figure 4.2).

Measured variables:

T_{301}	condenser inlet temperature [^{o}C]
T_{302}	condenser outlet temperature [^{o}C]
$\dot{m}_4$	secondary fluid flow in the condenser [kg/s]

Calculated variables:

$\bar{c}_p \approx f(0.5(T_{301} + T_{302}))$	liquid average heat capacity [J/kg.K], [6]

The condenser capacity is obtained from:

$$\dot{Q}_{cd} = \dot{m}_4 \bar{c}_p (T_{302} - T_{301}) \tag{4.19}$$

4.4.6 Compressor work

The compressor work delivered to the fluid is calculated from the suction and discharge enthalpies and the compressor mass flow-rate.

Measured variables:

T_{14}	compressor suction temperature [^{o}C]
T_1	compressor discharge temperature [^{o}C]
$\dot{m}_1$	refrigerant flow through compressor [kg/s]
p_{11}	system's low absolute pressure [Pa]
p_8	system's high absolute pressure [Pa]

Estimated variables: Pressure losses in tubes

Calculated variables:

$h_{14} = f(T_{14}, p_{14})$	vapour refrigerant enthalpy [J/kg], REFPROP, [7]
$h_1 = f(T_1, p_1)$	liquid refrigerant enthalpy [J/kg], REFPROP

The compressor work is calculated from:

$$\dot{W}_{cp} = \dot{m}_1 (h_1 - h_{14}) \tag{4.20}$$

4.4.7 Experimental energy balance checks

The energy balance checks are an application of the energy conservation law to the experimental results. Energy balance checks are applied in the experimentation for the components where the measured quantity can be determined from additional independent measurements. The results for the measured quantity, obtained from the independent measurements must agree within their uncertainty intervals. In the present experimentation this has been done in the tests of air-cooling compact heat exchangers using liquid and phase-changing refrigerant, and for the condenser in the liquid overfeed system.

The utility of the balance checks in the control of the experimental quality is obvious. In the initial phase of the experiment they can help to determine if some errors in the measurements have not been taken into account in the uncertainty analysis. In the execution phase the experimental balance checks permit to control and verify the quality of the experimental results, and detect possible failures in the instrumentation or the process control.

A balance check for experimentally determined cooling capacities of air-cooling heat exchanger is schematically represented in Figure 4.3.

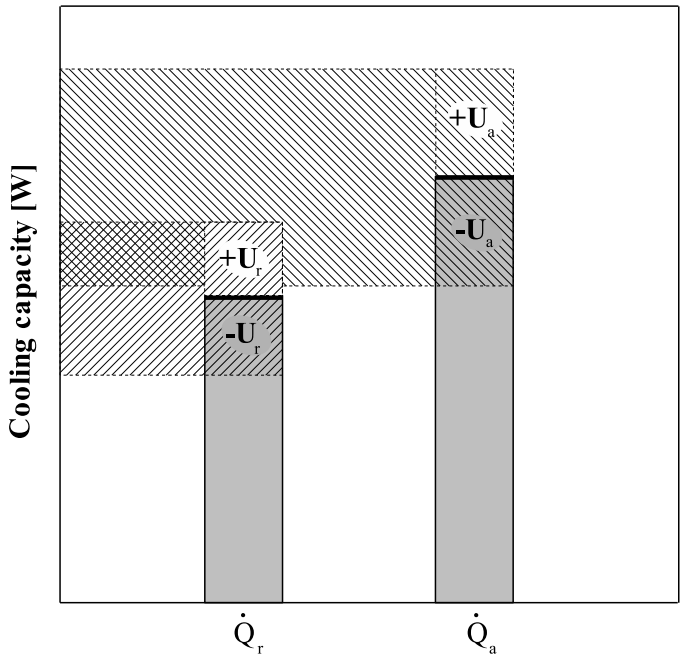

Figure 4.3: Schematic balance check for the experimental cooling capacity

4.5 Measuring uncertainty formulation and analysis

The objective of the experimental work is the obtaining of some result, usually based on measurements of different variables, combined in some expression called data reduction equation, that could be generically written in the form:

$$R = R(\bar{X}_1, \bar{X}_2, ..., \bar{X}_J) \tag{4.21}$$

where R is the experimental result determined from J measured variables $\bar{X}_i$ which are average values of N readings. Each of the measured variables contains systematic errors and random errors, estimated respectively with their systematic and random uncertainties. These uncertainties in the measured values then propagate through the data reduction equation, thereby generating systematic and random uncertainty of the result R.
The derivation of the uncertainty propagation equation is presented by Coleman and Steele in [8] together with additional assumptions for engineering applications. This methodology has been adopted in this work. It is consistent with the mathematical procedures of the ISO Guide [3] and is the recommended by the AIAA standard [9].
The uncertainty in the result is determined from:

$$U_r^2 = B_r^2 + P_r^2 \tag{4.22}$$

where B_r and P_r represent respectively the systematic and the random uncertainties in the result.
The systematic uncertainty of the result is:

$$B_r^2 = \sum_{i=1}^{J} \theta_i^2 B_i^2 + 2 \sum_{i=1}^{J-1} \sum_{k=i+1}^{J} \theta_i \theta_k B_{ik} \tag{4.23}$$

where the partial derivative $\theta_i = \partial R / \partial X_i$ is the sensitivity of the result R with respect to the measurement X_i and is computed numerically, sequentially perturbing the arguments of the data reduction equation (4.21) as suggested by Moffat [2]; B_i is the systematic uncertainty of the variable X_i; and B_{ik} is the correlated systematic uncertainty. The systematic uncertainty B_i of the individual variable is a result of a number of elemental sources of systematic uncertainty, such as calibration uncertainty, data acquisition uncertainty, data reduction, test techniques. The systematic uncertainty of the i-th variable can be calculated from the root-sum-square (RSS) combination of the M recognized as significant elemental uncertainties:

$$B_i = \Big[\sum_{k=1}^{M} (B_i)_k^2 \Big]^{1/2} \tag{4.24}$$

The correlated systematic uncertainty is calculated as proposed by Brown et al. [10]:

$$B_{ik} = \sum_{\alpha=1}^{L} (B_i)_\alpha (B_k)_\alpha \tag{4.25}$$

where L is the number of elemental systematic error sources that are common for measurements of variables X_i and X_k.
The random uncertainty of the result P_r is given from:

$$P_r^2 = \sum_{i=1}^{J} \theta_i^2 P_i^2 \tag{4.26}$$

assuming no correlated random uncertainties. The random uncertainties P_i of the variables X_i are determined directly from the experimental data. When N is the number of readings in the current experimental data, the sample standard deviation is:

$$s_{x_i} = \left[\frac{1}{N-1} \sum_{k=1}^{N} \left[(x_i)_k - \bar{\mathrm{X}}_i \right]^2 \right]^{\frac{1}{2}} \tag{4.27}$$

where

$$\bar{\mathrm{X}}_i = \frac{1}{N} \sum_{k=1}^{N} (x_i)_k \tag{4.28}$$

The sample standard deviation of the mean is:

$$S_{\bar{X}_i} = s_{x_i} / \sqrt{N} \tag{4.29}$$

The 95% confidence random uncertainty for a variable X_i is estimated as:

$$P_i = t S_{\bar{X}_i} \tag{4.30}$$

where t is the 95% confidence level value of the Student's t-distribution for $N-1$ degrees of freedom. For large samples containing more than 30 readings, $t = 2$ is assumed. For smaller samples the appropriate value of t is used.

Considerations for the uncertainty analysis

The systematic uncertainty B_i of the temperature measuring instruments after calibration is determined from comparison with a reference precision thermometer, as described in the section treating calibration, and comprises calibration errors and data acquisition errors. The systematic uncertainty of the other measuring instruments,

which are factory calibrated, is obtained from equation (4.24) summing the calibration and data acquisition uncertainties according to the root-sum-square (RSS) rule. Correlation of the errors of voltage and resistance measurements in different channels of the data acquisition system have not been observed, so they have been considered independent measurements.
The errors introduced from the data acquisition system are relatively small, except for the thermo-couple (TC) measurements. The main sources of error after calibration are introduced from temperature gradients in the isothermal block and the reference temperature for the TC. In the errors of TC measurements have been observed some correlation for those that are sharing the same multiplexor module. In controlled ambient have been observed that the thermo-couples connected to the same module show values consistently higher or lower than those of the precision thermometer. The explanation of this is that all the reference TC junctions in the multiplexor module are connected to the same isothermal block and its temperature is measured with the same sensor of reference. Error in the measurement of that reference temperature leads to a consistent error in the measurements of all the thermo-couples related to that reference. For this reason the errors in the measurements of all the TC connected to the same multiplexor are considered fully correlated to the extent of the data acquisition error, which is $\pm 0.2^oC$. This affects especially the cases where average temperature is calculated from these measurements.

4.6 Data corrections

Corrections for radiation are introduced to the measurements of the thermo-couples measuring the air temperature near the heat exchanger. The radiation exchange between the measuring thermo-couple and the surrounding walls is calculated considering it as a sphere within a parallelepiped formed from the surrounding walls. One of the walls (the cold wall) is formed by the cooling coil, the other are the duct walls and the droplet eliminator. As an estimate of the cold wall temperature is taken the tube temperature nearest to the TC, given by the numerical simulation, and the other walls are considered to be at the averaged air temperature measured by the thermo-couples in the air cross-section. Emissivities of black body are considered ($\varepsilon = 1$). View factors for each TC considering its geometrical location are calculated [11]. The radiosity (J) and the irradiation (G) are calculated using iterative Gauss-Seidel algorithm from:

$$G_i = F_{i1}J_1 + F_{i2}J_2 + F_{i3}J_3 + F_{i4}J_4 + F_{i5}J_5 + F_{i6}J_6 + F_{i7}J_7 \quad (4.31)$$

$$J_i = \sigma\varepsilon_i T_i^4 + \rho_i G_i \quad (4.32)$$

where $i = 1, 2, ..., 7$.

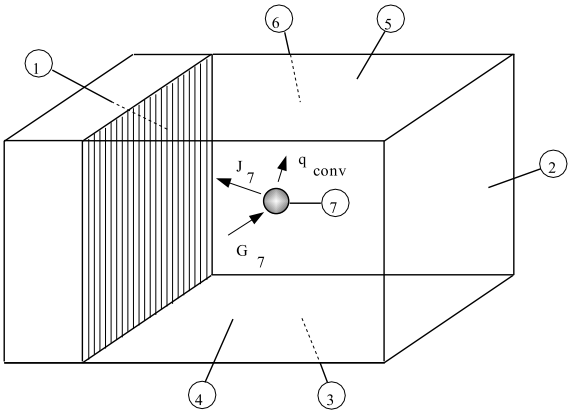

Figure 4.4: Radiation exchange between the thermo-couple and the surroundings

The convective heat transfer coefficient between the thermo-couple and the air is determined from empirical correlation taken from [12].
From the energy balance over the thermo-couple the temperature correction is determined.

$$\dot{q}_{conv} = \alpha(T_{air} - T_{TC}) \tag{4.33}$$

$$J_7 - G_7 + \dot{q}_{conv} = 0 \tag{4.34}$$

$$\Delta T_{corr} = T_{air} - T_{TC} = \frac{J_7 - G_7}{\alpha} \tag{4.35}$$

$$T_{air} = T_{TC} + \Delta T_{corr} \tag{4.36}$$

The analysis of the radiative heat transfer influence over the thermo-couple measurements have shown to be insignificant for the most of the studied cases. The maximum temperature correction applied has been of 0.06^oC.

4.7 Data processing

The obtained experimental information from the test records is processed and analysed to obtain the experimental results, and to perform the experimental to numerical comparisons. The great amount of information required the development of software tools that permit automated data reduction, analysis and comparison.
In a previous step, the experimental test records are processed with a specially developed software tool in order to obtain statistical resume files for each test point. This files contain the average values of the variables, the maximum and minimum values, and the standard deviation for each variable during the test. These statistical files are

used in the later data analysis, and for generation of the input files for the numerical simulation of the tested prototypes at the exactly same experimental conditions. The numerical simulations are performed and their output is stored for comparison with the experimental results. The numerical simulation output files contain detailed information, as the cooling capacity, the outlet temperatures of the air and refrigerant, the pressure drops air- and refrigerant-side. In wet cases (with humidity condensation over the heat exchanger) the water condensation rate is given. In cases of experiments with phase-changing refrigerant (evaporators), the vapour quality at the outlet is available.

The data reduction, uncertainty analysis, balance checks, and experimental-numerical comparisons are done automatically with a program written in Perl for this purpose. A list of all statistical and numerical simulation output files is passed to the program. The program opens these files and loads the data used in the processing.

The data processing and analysis are performed from different modules within the Perl program. The physical properties module calculates the physical properties of the liquid refrigerants and the air, and incorporates psychrometrical relations. The properties of the phase-changing refrigerants proportioned by REFPROP [7] are obtained calling external programs written in C language. The experimental cooling capacities air- and refrigerant-side are obtained using the formulation exposed in section 4.4. The uncertainty analysis is performed following the methodology described in section 4.5, with the exposed considerations. The systematic uncertainties of the measuring instruments are obtained in a previous step as described in section 4.3. The random uncertainties are determined as explained in section 4.5 directly from the measuring data assuming $t = 2$ for 95% confidence level. The sensitivity coefficients (partial derivatives) in the uncertainty propagation equations are obtained numerically, sequentially perturbing the variables in the data reduction equations from which the experimental cooling capacities are calculated, as suggested in [2]. The overall uncertainties (U) in the cooling capacities are obtained summing the systematic (B) and random uncertainties (P), using RSS for each test point. The overall uncertainty in each result varies from test to test, depending on the range of the measured variables, temperature differences and process steadiness.

Once the experimental cooling capacities air- and refrigerant-side are calculated, together with their uncertainties, these are cross-checked to verify their agreement within their corresponding uncertainty intervals. The reported experimental cooling capacity is calculated as an algebraic mean of the capacities obtained air- and refrigerant-side, $\dot{Q}_{exp} = 0.5(\dot{Q}_r + \dot{Q}_a)$, and its uncertainty is calculated.

Afterwards experimental to numerical results' comparisons are performed. These comparisons are done in four aspects: heat transfer, pressure drop air-side, pressure drop refrigerant-side and water vapour condensation rate for the wet cases. Statistical analysis is carried out in order to determine the mean numerical to experimental

difference and its respective dispersion for all the cases, and for groups of cases divided according to air velocity, refrigerant velocity, wet and dry cases. This is done in order to reveal if some relation exists between the magnitude of the experimental to numerical differences and the specific working conditions.
The data processing and analysis program generates an extensive output. It consists of data presented in tabular form and data files in convenient format for graphical presentation.

4.8 Conclusions

This chapter has been dedicated to the preparation of the measuring instrumentation, the test procedures and the subsequent data processing and experimental uncertainty analysis.
Concepts and terminology concerning experimentation and uncertainty analysis have been introduced, commented and adopted. Special attention has been put to the calibration of the measuring instruments, as an essential part of the test preparation. The process of estimation of the systematic uncertainties in the calibrated sensors measurements is described. For the factory calibrated instruments, an analytical approach in evaluation the systematic uncertainty is used, based in the root-sum-squaring of the calibration and data acquisition uncertainties. For the temperature sensors, calibrated in the CTTC versus precision thermometer, experimental procedure for evaluation of the remaining uncertainties is presented.
The obtaining of the experimental results from the measured variables during the experiment is presented in a separate section. The formulation for obtaining the cooling capacity of the tested compact heat exchangers both air- and refrigerant-side is exposed. The formulation for determining of the condenser capacity and the compressor work in the experimental liquid overfeed refrigeration system is also presented. The concept of the experimental balance checks is introduced and their application in the experiments is commented.
The uncertainty formulation and analysis adopted for the purpose of the present experimentation is presented, and the considerations about the different instruments are exposed.
Finally, the experimental processing and analysis program, specially developed for automated obtaining of the experimental results, the experimental uncertainties, and for comparison of the experimental and numerical results, is presented.

4.9 Nomenclature*

B	systematic uncertainty
G	irradiation $[W/m^2]$
J	radiosity $[W/m^2]$
N	number of readings in sample
P	random uncertainty
$\dot{q}$	heat flux per unit surface $[W/m^2]$
$\dot{Q}$	heat flux $[W]$
R	result, generic
s	sample standard deviation
S	sample standard deviation of the mean
t	Student's t-distribution value 95% confidence
T	temperature $[K]$
U	uncertainty of experimental result
X	measured variable

Greek symbols

α	convective heat transfer coefficient $[W/m^2K]$
β	systematic (fixed) component of the total error
δ	total measurement error
ΔT	temperature difference $[K]$
ε	emissivity
ϵ	random (variable) component of the total error
θ	partial derivative or sensitivity
ρ	reflectivity
σ	standard deviation of a parent population, Steffan Bolzman's constant 5.67×10^{-8} $[W/m^2K^4]$

Subscripts

a, air	air
acq	acquisition
cal	calibration
$conv$	convective
$corr$	correction
i	index of measured variable or sensor
max	maximum
pr	precision thermometer
r	result, refrigerant
TC	thermo-couple

Superscripts

$diff$	difference

Abbreviations

$CTTC$	Centre Tecnològic de Transferència de Calor
PT	precision thermometer
RSS	root-sum-square
RTD	resistance thermal device
TC	thermo-couple

* Note: For convenience, the nomenclature of section 4.4 is given within the text.

References

[1] Hugh W. Coleman and W. Glen Steele. *Experimentation and Uncertainty Analysis for Engineers*. John Wiley & Sons, 1989.

[2] Robert J. Moffat. Describing uncertainties in experimental results. *Experimental Thermal and Fluid Science*, vol.1:pp.3–17, 1988.

[3] International Organization for Standardization. *Guide to the Expression of Uncertainty in Measurement*, Geneva, Switzerland, 1993.

[4] ASME Standard PTC 19.1-1998. *Test Uncertainty*, 1998.

[5] ASHRAE. *Fundamentals Handbook*. 1993.

[6] Masao Furukawa. Practical expressions for thermodynamic and transport properties of commonly used fluids. *Journal of Thermophysics*, 1991.

[7] National Institute of Standards and Technology. *NIST Thermodynamic and Transport Properties of Refrigerants and Refrigerant Mixtures - REFPROP v6.01.*, Gaithersburg, MD, USA, 1998.

[8] Hugh W. Coleman and W. Glen Steele. Engineering application of experimental uncertainty analysis. *AIAA Journal*, vol.33(no.10):pp.1888–1896, October 1995.

[9] AIAA Standard S-071-1995. *Assessment of Wind Tunnel Data Uncertainty*, Washington, DC, June 1995.

[10] Kendall K. Brown, H. W. Coleman, W. G. Steele, and R. P. Taylor. Evaluation of correlated bias approximations in experimental uncertainty analysis. *AIAA Journal*, vol.34(no.5):pp.1013–1018, May 1996.

[11] Michael F. Modest. *Radiative Heat Transfer*. McGraw-Hill, 1993.

[12] H.Y.Wong. *Handbook of Essential Formulae and Data on Heat Transfer for Engineers*. Longman, 1977.